Condensates in double-well potential with synthetic gauge potentials and vortex seeding

Rukmani Bai
Physical Research Laboratory, Navrangpura, Ahmedabad-380009, Gujarat, India
Indian Institute of Technology, Gandhinagar, Ahmedabad-382424, Gujarat, India

Arko Roy
Physical Research Laboratory, Navrangpura, Ahmedabad-380009, Gujarat, India
Max-Planck-Institut für Physik komplexer Systeme, Nöthnitzer Straße 38, 01187 Dresden, Germany

D. Angom
Physical Research Laboratory, Navrangpura, Ahmedabad-380009, Gujarat, India

P. Muruganandam
School of Physics, Bharathidasan University, Tiruchirapalli 620 024, Tamil Nadu, India
(Dated: July 23, 2018)

We demonstrate an enhancement in the vortex generation when artificial gauge potential is introduced to condensates confined in a double well potential. This is due to the lower energy required to create a vortex in the low condensate density region within the barrier. Furthermore, we study the transport of vortices between the two wells, and show that the traverse time for vortices is longer for the lower height of the well. We also show that the critical value of synthetic magnetic field to inject vortices into the bulk of the condensate is lower in the double-well potential compared to the harmonic confining potential.

arXiv:1705.06493v2 [cond-mat.quant-gas] 20 Jul 2018

I. INTRODUCTION

Charged particles experience Lorentz force in the presence of magnetic fields, and in condensed matter systems, it is the essence for a host of fascinating phenomena like the integer quantum Hall effect [1, 2], fractional quantum Hall effect [3, 4], and the quantum spin Hall effect [5]. In contrast, the dilute quantum gases of atoms, which have emerged as excellent proxies of condensed matter systems, do not experience Lorentz force as these are charge neutral. This can, however, be remedied with the creation of artificial gauge fields through laser fields [6–10]. Thus, with the artificial gauge potentials it is possible to explore phenomena such as the quantum Hall effect, and the quantum spin Hall effect [7] in dilute atomic quantum gases. The introduction of synthetic magnetic field arising from artificial gauge field is also an efficient approach to generate quantized vortices in Bose-Einstein condensates (BEC) of dilute atomic gases. This method has the advantage of having time-independent trapping potentials over the other methods like rotation [11–13], topological phase imprinting [14, 15], or phase engineering in two-species condensates[16, 17]. In addition, it has the possibility to inject large ensembles of vortices, and an efficient scheme to nucleate vortices with synthetic magnetic fields was demonstrated in a recent work [18]. The method relies on the creation of an inhomogeneous synthetic magnetic field, which has its maxima coincident with the low density region of a spatially separated pair of BECs.

In this work we examine a scheme to nucleate vortices in BECs through synthetic magnetic field by employing the density gradient associated with a double well trapping potential. The advantages of the scheme are: vortices are generated in the bulk of the condensate; shorter relaxation time after nucleation; and higher density of vortices. In contrast, the other methods like rotating traps and phase imprinting nucleates vortices at the periphery. These then migrate to the bulk and as the process is diabatic, the relaxation times are long. Hence, the present scheme is better suited to explore phenomena associated with high vortex densities like quantum turbulence [19, 20]. BECs in double well potentials were first theoretically studied to examine the physics of Josephson currents [21–23], latter observed in experiments [24–27], and studied numerically in a recent work[28]. For our study, we theoretically consider the case of a double well potential which is engineered from a harmonic potential by introducing a Gaussian barrier. For alkali metal atoms the barrier is a blue-detuned light sheet obtained from a laser beam, and such setups have been used in experiments to observe the matter wave interference [29], Josephson effects [26] and collision of matter-wave solitons [30]. The artificial gauge potential is introduced through Raman coupling [8], and as a case study we consider the case of ^{87}Rb BEC. We use Gross-Pitaevskii (GP) equation for a mean-field description of the BEC with the artificial gauge potential. In this work we quench the artificial gauge potential by increasing the Raman detuning, and simultaneously increase the height of the barrier potential. It is found that the extended low density region associated with the barrier promotes the formation of vortices. However, the quench imparts energy to the BEC and transfer it to an excited state. For comparison, we also examine the vortex generation in the case of uniform BEC [31]. Such a system, devoid of trap induced inhomogeneities, is better for quantitative comparison of experimental results with theory. This was demonstrated in a recent study on wave turbulence in uniform BECs [32]. To induce relaxation of the condensate to the ground state, we use the standard approach of introducing a dissipative term [33–35]. The presence of the dissipative term in the GP equation is consistent with the experimental observations of dissipation or damping [36, 37], which arises from the in-

teraction between the condensate and non-condensate atoms.

The paper is organized as follows, in Section. II we provide a description of the theory on how to generate artificial gauge potential in BECs using Raman coupling. Then, we incorporate the gauge potential in the Gross-Pitaevskii equation to arrive at a mean field description of BEC. In Section. III, we present the results of numerical computations, and discuss the implications. We, then, conclude with the key observations.

II. BEC IN ARTIFICIAL GAUGE POTENTIALS

To study the vortex formation in double well with synthetic magnetic field in BECs theoretically, we consider the scheme based on light induced gauge potential proposed in ref. [8]. In particular, we consider a quasi-2D BEC along the xy-plane of two level atoms, which in the present work is taken as the $F = 1$ ground state of ^{87}Rb atoms. To generate spatial inhomogeneity an external magnetic field $B(y) = B_0 + \Delta B(y)$ is applied along the y direction. Here B_0 is the static magnetic field which introduces a linear Zeeman splitting of the ground state manifold. The energy levels are separated by $\Delta_{\rm z} = g\mu_{\rm B}B_0$, and $\delta(y) = g\mu_{\rm B}\Delta B(y)$ is the measure of detuning from Raman resonance. The constants g and $\mu_{\rm B}$ are the atomic Landé factor and Bohr magneton, respectively. The two levels in the ground state are Raman coupled through two counter-propagating laser beams passing through the BEC along $\pm x$ directions [38]. The momentum transferred to the atoms through interactions with the Raman lasers induces a change in the kinetic energy part of the Hamiltonian through the vector potential term A_x. The modified Hamiltonian, however, remains gauge invariant, and there is a corresponding synthetic magnetic field $B_z = -\partial A_x/\partial x$.

A. Modified Gross-Pitaevskii equation

In the absence of Raman coupling, the Hamiltonian of the quasi-2D BEC confined in an harmonic trapping potential $\hat{V}_{\rm trap}$ is

$$\hat{H} = \hat{H}_x + \hat{H}_y + \hat{V}_{\rm trap} + \hat{H}_{\rm int}, \tag{1}$$

where $\hat{H}_x, \hat{H}_y$ represent the kinetic energy part of the Hamiltonian term along x, y directions respectively, and $\hat{H}_{\rm int}$ denotes the interaction energy between the atoms. Let $|1\rangle = |1, 0\rangle$ and $|2\rangle = |1, -1\rangle$ denote the two states in the ground state manifold of the atoms. The Raman lasers are along the x direction, and hence, the addition of the atom-light coupling term modifies H_x to

$$\hat{H}_x = E_{\rm r}\begin{pmatrix} \left(\tilde{k}_x + 1\right)^2 - \dfrac{\hbar\delta}{2E_{\rm r}} & \dfrac{\hbar\Omega}{2E_{\rm r}} \\ \dfrac{\hbar\Omega}{2E_{\rm r}} & \left(\tilde{k}_x - 1\right)^2 + \dfrac{\hbar\delta}{2E_{\rm r}} \end{pmatrix}, \tag{2}$$

where $E_{\rm r} = \left(\hbar^2 k_{\rm r}^2/2m\right)$ is the recoil energy, and $\tilde{k}_x = (k_x/k_{\rm r})$ with k_x as the x-component of the wave-vector, Ω is the Raman coupling between two levels, and δ is the Raman detuning.

To derive the modified Gross-Pitaevskii (GP) equation, we diagonalize $\hat{H}_x$ and obtain the dispersion relation for the two levels in the limit of strong Rabi coupling, $\hbar\Omega \gg 4E_r$. This ensures that there is single energy minima of the system and lead to the following: there is a change in the momentum along the x direction which provide a gauge potential $eA_x/\hbar k_{\rm r} = \tilde{\delta}/(\tilde{\Omega} \pm 4)$ in the system; and from the light-atom coupling the atoms acquires an effective mass m^* defined by $m^*/m = \tilde{\Omega}/(\tilde{\Omega} \pm 4)$. Here $\pm$ denotes the two energy levels in the system and $\tilde{\delta} = \hbar\delta/E_r$, $\tilde{\Omega} = \hbar\Omega/E_r$. Based on this Hamiltonian and restricting the dynamics to only the lowest dressed state, the behaviour of such a condensate in the presence of artificial gauge fields is governed by the following dimensionless modified Gross-Pitaevskii (GP) equation

$$\begin{aligned} i\frac{\partial\phi(x,y,t)}{\partial t} = \Bigg[& -\frac{1}{2}\frac{m}{m^*}\frac{\partial^2}{\partial x^2} - \frac{1}{2}\frac{\partial^2}{\partial y^2} + \frac{i2\pi\delta^{'}}{\lambda_{\rm L}\Omega E_{\rm r}} y\frac{\partial}{\partial x} \\ & + \frac{1}{2}x^2 + \frac{1}{2}y^2\left(1 + \frac{2C_{\rm rab}\delta^{'2}}{E_{\rm r}}\right) + g_{\rm 2D}|\phi(x,y,t)|^2 \\ & - \left(\frac{\Omega - 2}{2}\right)E_{\rm r}\Bigg]\phi(x,y,t). \end{aligned} \tag{3}$$

In the above equation, all the parameters having the dimensions of length, energy, and time have been scaled with respect to the oscillator length $a_{\rm osc} = \sqrt{\hbar/m\omega_x}$, energy $\hbar\omega_x$ and time $\omega_x t$ respectively. For simplicity of notations, from here on we will represent the transformed quantities $(\Omega, \delta^{'}, E_{\rm r}, \lambda_{\rm L})$ without tilde. The condensate wavefunction is represented by $\phi(x, y, t)$, $C_{\rm rab} = \left(1/\Omega(\Omega - 4) + (4 - \Omega)/4(\Omega + 4)^2\right)$, $\delta = \delta^{'}y$, $\delta^{'}$ is defined to be the detuning gradient, Ω is the Rabi frequency, $E_{\rm r} = \left(2\pi^2/\lambda_{\rm L}^2\right)$ is the recoil energy of electrons, $g_{\rm 2D} = 2a_s N\sqrt{2\pi\lambda}/a_{\rm osc}$ is the interaction energy with N as the total number of atoms in the condensate, and $\lambda \gg 1$ is the trap anisotropy parameter along the z direction.

B. Double Well (DW) Potential

For the present work, we consider quasi-2D BEC confined in a double well potential

$$V_{\rm dw} = V_{\rm trap} + U_0 \exp(-2y^2/\sigma^2), \tag{4}$$

where U_0 and σ are the depth and width of the double well potential respectively and $V_{\rm trap} = (1/2)m\omega_\perp^2(x^2 + y^2)$ is the harmonic potential along x and y directions, and we have considered the symmetric case $\omega_\perp = \omega_x = \omega_y$.

The presence of the double well potential modifies the density distribution, breaks the rotational symmetry of the condensate, and brings about novel effects in the dynamical evolution of the condensate which forms the main topic of the present study.

C. Thomas Fermi Correction in the condensates density

The focus of the present work, as mentioned earlier, is to examine the formation of vortices in the quasi-2D BEC with the introduction of artificial gauge potential. It has been shown in previous works on rotated condensates that vortices are seeded at the periphery of the condensate cloud, where the low density of the condensate is energetically favourable for the formation of vortices [39]. This is due to the presence of nodeless surface excitations [40], which create instabilities in the condensate and lead to the nucleation of vortices [41]. At later times the vortices migrate and enter the bulk of the condensate. To analyse the density distribution and optimal conditions for generation of vortices, consider a BEC with large number of particles. The condensate is then well described with the Thomas-Fermi (TF) approximation as the interaction energy dominates in the GP equation, and the kinetic energy can be neglected in the bulk of the condensates as the spatial gradient is negligible. In this approximation the density in the bulk is $|\phi_{\rm TF}|^2 = (\mu - V_{\rm trap})/(2g_{2D})$, where μ is the chemical potential of the condensate. The TF approximation, however, fails at the periphery of condensate as the $\phi_{\rm TF}$ is discontinuous at the boundary [42]. However, vortices are seeded at the peripheral regions where the TF approximation may break down. Similar conditions are applicable to the densities at the edges of the double well potential considered in the present work. For this we take μ in terms of TF radius R and trapping potential in term of radial distance r. The correction to the TF density at the edges, similar to the harmonic trapping potential, is

$$|\phi^c_{\rm TF}|^2 = \frac{R^2 - r^2}{2g_{2D}}\Big[1 - \frac{R^2}{2(R^2 - r^2)^3}\Big]^2. \qquad (5)$$

In the above equation, first term is TF density in the bulk of condensate and second term is correction to the TF density. Now, the density at the boundary is calculated as $n_c = |\phi_{\rm TF}|^2 - |\phi^c_{\rm TF}|^2$, and for the region within the barrier of the double well, TF approximation is valid as the barrier potential decays exponentially. Accordingly, the density distribution is

$$|\phi^b_{\rm TF}|^2 = \frac{R^2 - r^2 - U_0 \exp(-2y^2/\sigma^2)}{2g_{2D}}, \qquad (6)$$

here U_0 and σ are depth and width of the double well potential. The above density distribution is symmetric about the x-axis, and hence, the low density region is more extended compared to the peripheral region of a harmonic trapping potential. So, the density variation arising from the potential barrier enhances the formation of vortices.

III. RESULTS AND DISCUSSION

A. Numerical details

For the present study, we numerically solve the Gross-Pitaevskii equation in imaginary time at zero temperature in the absence of the artificial gauge potential, which is equivalent to setting $\delta^{'}$ and Ω to zero. For this we use the split-step Crank-Nicolson method [43–46] and the solution obtained is the equilibrium ground state. To dynamically evolve the condensate, we propagate the stationary state solution in real time using Eq. (3). Furthermore, we introduce the artificial gauge potential by varying $\delta^{'}$ from 0 to 3×10^9 Hz/m within ≈ 202 ms, but the value of Ω is kept constant throughout the evolution. Afterwards the system is evolved freely for up to $t \approx 962$ ms when it relaxes to a steady state. For the present work we consider ^{87}Rb condensate with $N = 10^5$ atoms, and the s-wave scattering length is $a_s = 99a_0$. The trapping potential parameters are chosen to be $\omega_x = \omega_y = 2\pi \times 20$ Hz, and $\lambda = 40$ which satisfies the quasi-2D condition. The Raman lasers considered for our calculations have wavelength $\lambda_{\rm L} = 790$ nm. The Rabi frequency is taken to be $\Omega = 6E_r$, where E_r is scaled with $\hbar\omega_x$. This choice of parameters is consistent with the experimental setting of Spielman *et al.*[8].

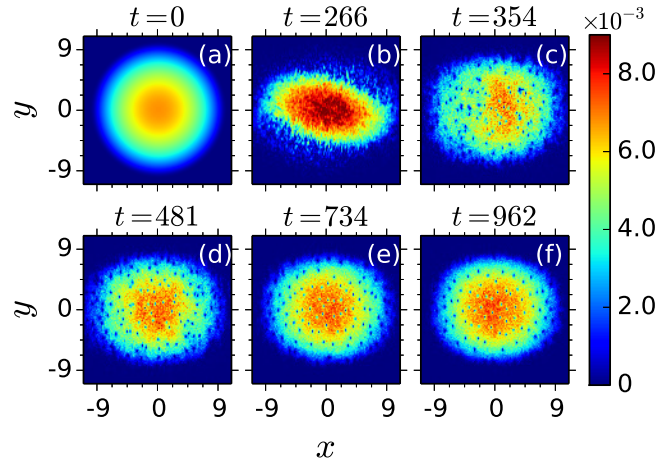

FIG. 1. Generation of vortices in the absence of dissipation. The time (in units of ms) is shown above the plots. Here x and y are measured in units of $a_{\rm osc}$. Density is measured in units of $a_{\rm osc}^{-2}$ and is normalized to unity.

B. Harmonic potential

At the start of the real time evolution, or beginning of the dynamical evolution $t = 0$, the condensate is rotationally symmetric, and is devoid of any topological defects. This is shown in Fig. 1(a). As the artificial gauge potential is switched on in by introducing $\delta^{'}$ with constant Ω, the rotational symmetry of the condensate is broken since the effective frequencies along x and y directions are unequal due to the term $2C_{\rm rab}\delta'^2/E_{\rm r}$ in Eq. (3). The condensate thus departs from being circularly symmetric and acquires an elliptic structure, which is discernible from the density profiles shown in Fig. 1. Furthermore, the angular-momentum like term $i(2\pi\delta')/(\lambda_{\rm L}\Omega E_{\rm r})(y\partial\phi(x,y,t))/(\partial x)$ in Eq. (3) is non-zero and induces a deformation to the condensate. The com-

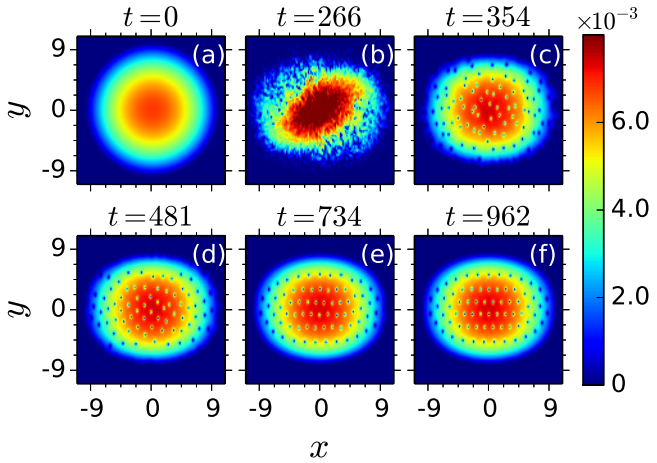

FIG. 2. Generation of vortices in the presence of dissipation. The time (in units of ms) is shown above the plots. Here x and y are measured in units of $a_{\rm osc}$. Density is measured in units of $a_{\rm osc}^{-2}$ and is normalized to unity.

bined effects of these two effects and an increase in the energy of the system favour the seeding of topological defects or vortices in the condensate. Initially, the vortices are generated at the periphery, where the density is low and fluctuations in phase are more prominent, and at later times the vortices migrate to the bulk of the condensate. As the system relaxes towards a steady state, the vortices acquires a spatially disordered distribution to minimize the total energy. The nature of the spatial distribution of vortices implies that the system is in a higher energy state, and this is evident from the vortex distribution as shown in Fig. 1(f). To include the effects of dissipation which may be present due to quantum and thermal fluctuations, or due to loss of atoms from the trap because of inelastic collisions in the condensate we add the dissipative term $-\gamma\partial\phi(x,y,t)/\partial t$ in Eq. (3) and examine the dynamical evolution of the condensate. Here, we set $\gamma = 0.003$ based on the results from previous work [35]. This leads to loss of energy from the condensate and the condensate dynamically evolves to it's ground state. As a consequence the vortices self organise into a vortex lattice and the evolution towards the vortex lattice is as shown in Fig. 2.

C. Double well potential

To study the dynamics of vortex generation and their transport in double well potential we solve time dependent GP Eq. (3) with the potential given in Eq. (4). Like in the previous case, we include a dissipative term to allow the system to relax to it's ground state, which is with a vortex lattice. For the numerical computation, we take the width of the barrier in the double well potential as $\sigma = 0.7\mu$m. To obtain the initial state, like in the previous case, we again consider imaginary time ground state solution of a quasi-2D BEC of ^{87}Rb atoms without δ', Ω, and U_0. We, then evolve the solution in real time as described earlier. During the evolution in real time, we ramp up or quench the value of δ' and U_0, but keeping Ω fix. Increment in δ' introduces artificial gauge potential in the system, and vortices are generated with time. We find that the double well potential has enhanced vortex formation. The vortices are generated in the barrier region between the two wells as it is a region of low density, and the energy per vortex is lower in this regime.

The enhancement of vortex formation in the double well potential can be understood in terms of the excitation energy of a single vortex. In the case of harmonic potential the energy of the vortex located at a radial distance b from the center in the TF approximation is $\epsilon_v \simeq (4/3)\pi R_z n(0)(\hbar^2/m)\ln(R/\xi_0)(1-b^2/R^2)^{3/2}$. Where, $n(0)$ is the density at the center, when vortex is not present, R is the Thomas-Fermi radius, R_z is the length along z direction and ξ_0 is the healing length [42]. For the quasi-2D system R_z can be evaluated using the anisotropy parameter λ and μ in the TF approximation. Based on this expression we find that the energy of a vortex at the center of the condensate with only the harmonic trapping potential or without the barrier is 0.028 $\hbar\omega_x$, which is lower than the value of 0.094 $\hbar\omega_x$ obtained from the numerical results. The difference could be due to deviation from the TF approximation. From the numerical results, without the barrier, the energy of a vortex located at a radial distance of 9.0 $a_{\rm osc}$ is 0.008 $\hbar\omega_x$. Here, the radial distance considered correspond to the peripheral region where vortices first appear. In the case of double well potential the energy of a vortex at the center of the barrier and at the same radial distance is 0.007 $\hbar\omega_x$, which is lower than the previous case. In terms of absolute values the energy difference is not large, but as discussed latter, the presence of the barrier in the double well makes a significant difference in the dynamical evolution and generation of vortices. Since we quench two parameters of the system, δ' and U_0, we examine the system in terms of the relative quench rates. For this we define $R_1 = \lambda_{\rm L}\partial\delta'/\partial t$ and $R_2 = \partial U_0/\partial t$ as the quench rate of the artificial gauge potential, and the barrier height between the two wells, respectively. Where $\lambda_{\rm L}$, δ', and U_0 are the dimensionless quantities, and δ' and U_0 are ramped within a period of $t = 202$ ms. The value of δ' vary from 0 to 3×10^9 Hz/m as defined earlier. Here, R_1 affects the vortex generation, and R_2 affects the transport of vortices between the two wells. We consider three cases, depending on the relative values of R_1 and R_2.

1. $R_1 < R_2$

For this case we vary U_0 from 0 to 25.85 (in units of $\hbar\omega_x$) within a period of 202 ms, and the evolution of the density profiles are shown in Fig. (3). The inclusion of the barrier, to form a double well potential, accelerates the formation of vortices, and they appear within a short span of time $\approx$ 40 ms. This is much shorter than the time of $\approx$ 266 ms taken to generate vortices in absence of the barrier or in harmonic potential as shown in Fig. (2). The shortening is due to the modified density distribution arising from the presence of the central barrier in the double well potential. The vortices are

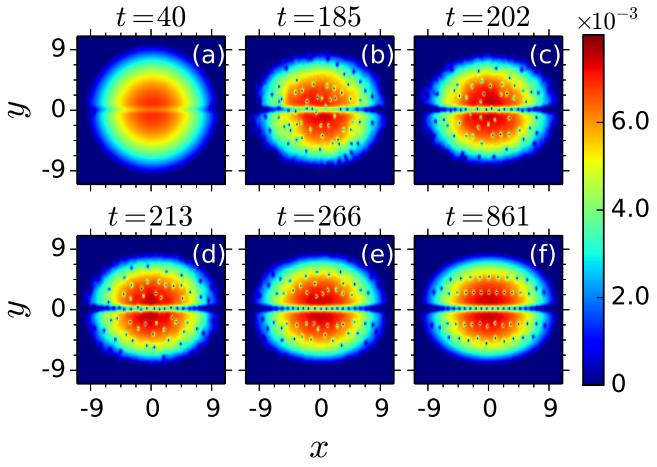

FIG. 3. Transport of vortices when laser field energy rate is less compared to the double well potential depth energy rate with dissipation. Vortices transport between the wells up to the time $t = 266$ ms, after that some vortices are settled near to the interface of the wells. The time (in units of ms) is shown above the plots. Here x and y are measured in units of $a_{\rm osc}$. Density is measured in units of $a_{\rm osc}^{-2}$ and is normalized to unity

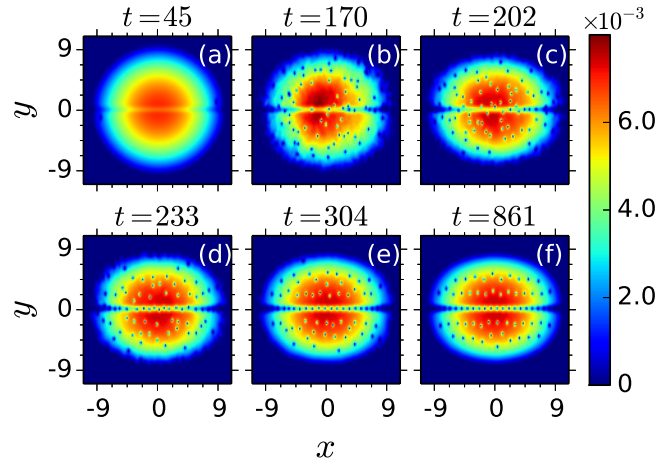

FIG. 4. Transport of vortices when laser field energy rate is equal to the double well potential depth energy rate with dissipation. Vortices cross from one well to another well up to the time $t = 304$ ms, after that some vortices are settled near the interface. The time (in units of ms) is shown above the plots. Here x and y are measured in units of $a_{\rm osc}$. Density is measured in units of $a_{\rm osc}^{-2}$ and is normalized to unity.

seeded near the central region of the barrier where the density is low as shown in Fig. (3) (a). During the quench, at lower values of U_0, vortices traverse from one well to the other due to the lower depth of the potential, but it stops once U_0 reaches maxima as the vortex energy is not enough for transport from one well to the other. The dynamics associated with the crystallisation of the vortices to form a vortex lattice is evident from the density patterns in Fig. (3) (b)-(e). The equilibrium ground state solution of vortex lattice is obtained at ≈ 861 ms after the free evolution as shown in Fig. (3) (f). One noticeable feature is the confinement of vortices along the barrier with lower spacing compared to the vortex lattice in the bulk of the condensate. In particular, the spacing between vortices is 1.43 $a_{\rm osc}$ and 0.87 $a_{\rm osc}$ in the bulk and in the barrier respectively.

2. $R_1 \geqslant R_2$

For the case of $R_1 = R_2$, the value of U_0 at the end of the quench is 18.85 (in units of $\hbar\omega_x$). During the quench vortices are generated at $\approx$ 45 ms of the dynamical evolution, and emerge from within the barrier region. Here, the potential depth is less compared to the case of $R_1 < R_2$, and the vortex transportation between the two wells occurs for a longer time, that is up to ≈ 304 ms. Like in the case of $R_1 < R_2$ the equilibrium ground state solution is attained at ≈ 861 ms. For illustration the condensate density profiles during the dynamical evolution are shown in Fig. (4). In the case of $R_1 > R_2$ the value of U_0 at the end of the quench is 11.85 (in units of $\hbar\omega_x$). This implies that the barrier height attained at the end of the quench is less than the two previous cases. The generation of vortices start at $\approx$ 50ms, and the transportation of vortices

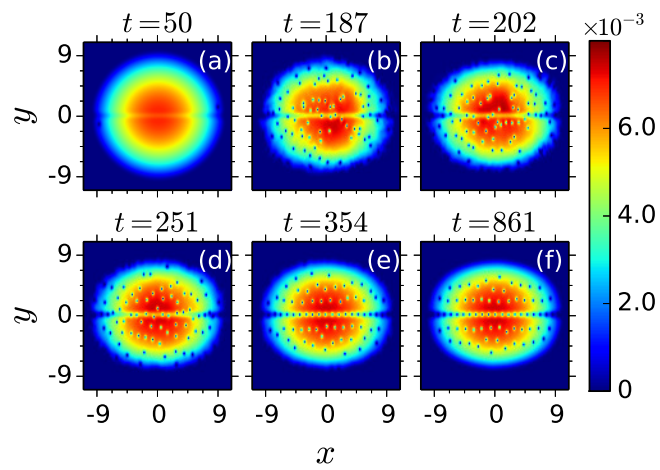

FIG. 5. Transport of vortices when laser field energy rate is high compared to the double well potential depth energy rate with dissipation. Vortices cross from one well to another well up to the time $t = 354$ ms, after that some vortices are settled near to the interface. The time (in units of ms) is shown above the plots. Here x and y are measured in units of $a_{\rm osc}$. Density is measured in units of $a_{\rm osc}^{-2}$ and is normalized to unity

between the two wells continues for much longer time, till ≈ 354 ms. Like in the previous cases the equilibrium ground state solution is obtained at ≈ 861 ms as shown in Fig. (5).

D. Uniform BEC

For uniform BEC, $V_{\rm trap}$ in Eq. 3 is set to zero and consider hard wall boundary. With this the BEC is uniform except at the boundary, where the density goes to zero over the length

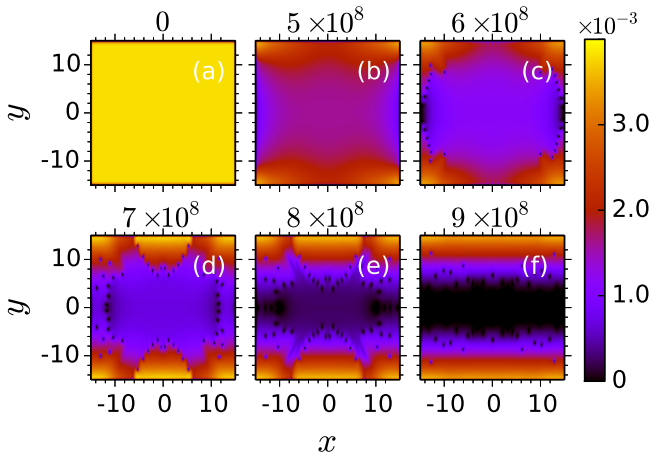

FIG. 6. Generation of vortices in the homogeneous system with the hard wall boundary with the synthetic magnetic field. The equilibrium solution for different value of $\delta^{'}$ (in Hz/m) are shown here and values of $\delta^{'}$ are written above each of the plot. Vortices are generated near to the boundary and propagate into the bulk of the condensate. Here x and y are measured in units of $a_{\rm osc}$. Density is measured in units of $a_{\rm osc}^{-2}$ and is normalized to unity

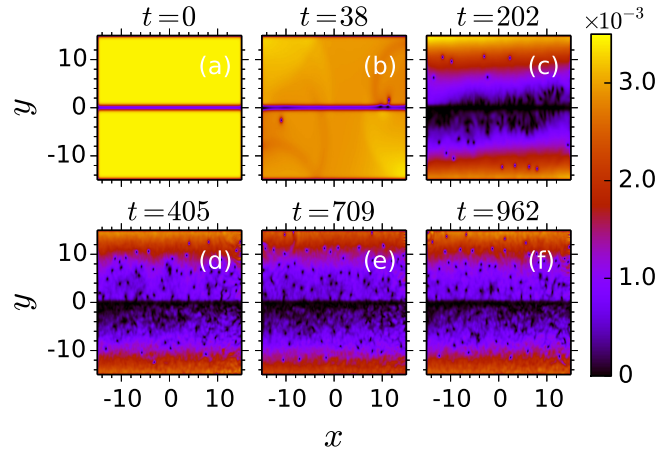

FIG. 7. Generation of vortices in the homogeneous system with the hard wall boundary. A barrier is introduced along the x direction. Vortices are generated near to the barrier and propagate into the bulk of the condensate. Here, we do not observe the vortex lattice. Here x and y are measured in units of $a_{\rm osc}$. Density is measured in units of $a_{\rm osc}^{-2}$ and is normalized to unity.

scale of healing length. So, the vortices enter from the edges and propagate to the bulk. We obtain the equilibrium state of the modified GP Eq. 3 with different values of synthetic magnetic field shown in the Fig. 6. We observe that condensate is fragmented at the large value of $\delta^{'} > 9 \times 10^8$ Hz/m. In this case there is no formation of vortex lattice. We find that the vortices have higher energies in the uniform BEC $\approx 10\ \hbar\omega_x$, whereas it is $\approx 3\ \hbar\omega_x$ for BEC with harmonic confining potential. The difference can accounted by the higher moment of inertia associated with the uniform BEC. Next, to compare with the results in presence of harmonic potential, we introduce a Gaussian barrier along x axis with $U_0 = 10$ (in units of $\hbar\omega_x$) and width of 0.7μm. In the numerical simulation, the initial states at time t = 0 ms is without the synthetic magnetic field $\delta^{'}$ = 0 as shown in Fig. 7(a). Then, the magnetic field is introduced by quenching $\delta^{'}$. The vortices are nucleated at a critical value of $\delta^{'}$ as shown in Fig. 7(b) at t = 38 ms. We increase $\delta^{'}$ from 0 to 7×10^8 Hz/m in 0 to 202 ms time. After that, we freely evolve the system. In the uniform BEC, like in the previous case, the vortices nucleate close to the barrier and then propagate to the bulk. However, as to be expected, the dynamics of the vortices are qualitatively different from the inhomogeneous case. The dynamics of the vortices are determined by the inter-vortex interactions and remain within the bulk regions. The selected snap shots of the dynamical evolution of the vortices are shown in the Fig. 7(a)-(f).

E. Critical value of $\delta^{'}$ and density

As described earlier, we take the equilibrium imaginary time solution of a quasi-2D BEC, and evolve it in real time with the introduction of a quenched artificial gauge potential. This is achieved by increasing the detuning gradient of the Raman lasers δ' and vortices are generated in the condensates when δ' reaches a critical value during the quench. In the case of a purely harmonic confining potential the critical value of δ' is 0.89×10^9 Hz/m. But, for the case of a condensate confined in double well potential the critical value of δ' is 0.26×10^9 Hz/m. Hence, the presence of the barrier in the double well potential lowers the critical value of δ', which is the measure of synthetic magnetic field in the system. To examine the generation of the vortices in more detail we examine the condensate density at the region where vortex enters in the condensate. In the case of harmonic trap, vortex enters from the peripheral region, and we use TF correction to compute the density n_c. We find that densities n_c for the two trapping potentials are 0.1×10^{-3} and 0.4×10^{-3} for the harmonic and double well potential. Here, densities are measured in units of $a_{\rm osc}^{-2}$ and are normalized to unity. These densities correspond to the region at which vortex enters in the condensates.

IV. CONCLUSIONS

We have shown that the presence of the Gaussian potential barrier enhances the generation of vortices due to the presence of artificial gauge potential. We examine this by quenching the artificial gauge potential along with the height of the barrier potential. Without the barrier potential, in the case of a harmonic confining potential, the vortices are generated at a later time and vortices are less in number as well. Like in the previous works [33–35], we observe that it is essential to introduce dissipation to obtain equilibrium vortex configuration

in trapped system. The dissipation drains energy gained during the quench and allows the condensate relax to the ground state configuration by forming a vortex lattice. In case of uniform BEC, there is no formation of vortex lattice even in the presence of dissipation.

ACKNOWLEDGMENTS

We thank Kuldeep Suthar, Sukla Pal and Soumik Bandopadhyay for very useful discussions. The numerical computations reported in the paper were carried on the Vikram-100 HPC cluster at PRL. The work of PM forms a part of Science & Engineering Research Board (SERB), Department of Science & Technology (DST), Govt. of India sponsored research project (No. EMR/2014/000644).

[1] K. von Klitzing, Rev. Mod. Phys. **58**, 519 (1986).
[2] D. R. Yennie, Rev. Mod. Phys. **59**, 781 (1987).
[3] H. L. Stormer, D. C. Tsui, and A. C. Gossard, Rev. Mod. Phys. **71**, S298 (1999).
[4] H. L. Stormer, Rev. Mod. Phys. **71**, 875 (1999).
[5] M. Knig, H. Buhmann, L. W. Molenkamp, T. Hughes, C.-X. Liu, X.-L. Qi, and S.-C. Zhang, J. Phys. Soc. Japan **77**, 031007 (2008).
[6] G. Juzeliūnas and P. Öhberg, Phys. Rev. Lett. **93**, 033602 (2004).
[7] S.-L. Zhu, H. Fu, C.-J. Wu, S.-C. Zhang, and L.-M. Duan, Phys. Rev. Lett. **97**, 240401 (2006).
[8] I. B. Spielman, Phys. Rev. A **79**, 063613 (2009).
[9] K. Jimenez-Garca, *Artificial Gauge Fields for Ultracold Neutral Atoms*, Ph.D. thesis, National Institute of Standards and Technology, and the University of Maryland Gaithersburg, Maryland (2012).
[10] N. Goldman, G. Juzelinas, P. Öhberg, and I. B. Spielman, Rep. Prog. Phys. **77**, 126401 (2014).
[11] K. W. Madison, F. Chevy, W. Wohlleben, and J. Dalibard, Phys. Rev. Lett. **84**, 806 (2000).
[12] J. R. Abo-Shaeer, C. Raman, J. M. Vogels, and W. Ketterle, Science **292**, 476 (2001).
[13] P. C. Haljan, I. Coddington, P. Engels, and E. A. Cornell, Phys. Rev. Lett. **87**, 210403 (2001).
[14] T. Isoshima, M. Nakahara, T. Ohmi, and K. Machida, Phys. Rev. A **61**, 063610 (2000).
[15] A. E. Leanhardt, A. Görlitz, A. P. Chikkatur, D. Kielpinski, Y. Shin, D. E. Pritchard, and W. Ketterle, Phys. Rev. Lett. **89**, 190403 (2002).
[16] J. E. Williams and M. J. Holland, Nature **401**, 568 (1999).
[17] M. R. Matthews, B. P. Anderson, P. C. Haljan, D. S. Hall, C. E. Wieman, and E. A. Cornell, Phys. Rev. Lett. **83**, 2498 (1999).
[18] R. M. Price, D. Trypogeorgos, D. L. Campbell, A. Putra, A. Valds-Curiel, and I. B. Spielman, New J. Phys. **18**, 113009 (2016).
[19] M. Tsubota, M. Kobayashi, and H. Takeuchi, Physics Reports **522**, 191 (2013).
[20] S. K. Nemirovskii, Physics Reports **524**, 85 (2013).
[21] J. Javanainen, Phys. Rev. Lett. **57**, 3164 (1986).
[22] F. Dalfovo, L. Pitaevskii, and S. Stringari, Phys. Rev. A **54**, 4213 (1996).
[23] A. Smerzi, S. Fantoni, S. Giovanazzi, and S. R. Shenoy, Phys. Rev. Lett. **79**, 4950 (1997).
[24] F. S. Cataliotti, S. Burger, C. Fort, P. Maddaloni, F. Minardi, A. Trombettoni, A. Smerzi, and M. Inguscio, Science **293**, 843 (2001).
[25] M. Albiez, R. Gati, J. Fölling, S. Hunsmann, M. Cristiani, and M. K. Oberthaler, Phys. Rev. Lett. **95**, 010402 (2005).
[26] S. Levy, E. Lahoud, I. Shomroni, and J. Steinhauer, Nature **449**, 579 (2007).
[27] A. Trenkwalder, G. Spagnolli, G. Semeghini, S. Coop, M. Landini, P. Castilho, L. Pezze, G. Modugno, M. Inguscio, A. Smerzi, and M. Fattori, Nat. Phys. **12**, 826 (2016).
[28] M. A. Garcia-March and L. D. Carr, Phys. Rev. A **91**, 033626 (2015).
[29] M. R. Andrews, C. G. Townsend, H.-J. Miesner, D. S. Durfee, D. M. Kurn, and W. Ketterle, Science **275**, 637 (1997).
[30] J. H. V. Nguyen, P. Dyke, D. Luo, B. A. Malomed, and R. G. Hulet, Nat Phys **10**, 918 (2014).
[31] A. L. Gaunt, T. F. Schmidutz, I. Gotlibovych, R. P. Smith, and Z. Hadzibabic, Phys. Rev. Lett. **110**, 200406 (2013).
[32] N. Navon, A. L. Gaunt, R. P. Smith, and Z. Hadzibabic, Nature **539**, 72 (2016).
[33] S. Choi, S. A. Morgan, and K. Burnett, Phys. Rev. A **57**, 4057 (1998).
[34] M. Tsubota, K. Kasamatsu, and M. Ueda, Phys. Rev. A **65**, 023603 (2002).
[35] D. Yan, R. Carretero-Gonzlez, D. J. Frantzeskakis, P. G. Kevrekidis, N. P. Proukakis, and D. Spirn, Phys. Rev. A **89**, 043613 (2014).
[36] M.-O. Mewes, M. R. Andrews, N. J. van Druten, D. M. Kurn, D. S. Durfee, C. G. Townsend, and W. Ketterle, Phys. Rev. Lett. **77**, 988 (1996).
[37] D. S. Jin, M. R. Matthews, J. R. Ensher, C. E. Wieman, and E. A. Cornell, Phys. Rev. Lett. **78**, 764 (1997).
[38] Y.-J. Lin, R. L. Compton, A. R. Perry, W. D. Phillips, J. V. Porto, and I. B. Spielman, Phys. Rev. Lett. **102**, 130401 (2009).
[39] E. Hodby, G. Hechenblaikner, S. A. Hopkins, O. M. Maragò, and C. J. Foot, Phys. Rev. Lett. **88**, 010405 (2001).
[40] U. A. Khawaja, C. J. Pethick, and H. Smith, Phys. Rev. A **60**, 1507 (1999).
[41] T. P. Simula, S. M. M. Virtanen, and M. M. Salomaa, Phys. Rev. A **66**, 035601 (2002).
[42] C. Pethick and H. Smith, *Bose-Einstein Condensation in Dilute Gases* (Cambridge University Press, 2008).
[43] P. Muruganandam and S. Adhikari, Comput. Phys. Commun. **180**, 1888 (2009).
[44] D. Vudragovi, I. Vidanovi, A. Bala, P. Muruganandam, and S. K. Adhikari, Comput. Phys. Commun. **183**, 2021 (2012).
[45] B. Satari, V. Slavni, A. Beli, A. Bala, P. Muruganandam, and S. K. Adhikari, Comput. Phys. Commun. **200**, 411 (2016).
[46] L. E. Young-S., D. Vudragovi, P. Muruganandam, S. K. Adhikari, and A. Bala, Comput. Phys. Commun. **204**, 209 (2016).